Variable Macropixel Spectral-Spatial Transforms with Intra- and Inter-color Decorrelations for Arbitrary RGB CFA-Sampled Raw Images

Taizo Suzuki, *Senior Member, IEEE*, and Seisuke Kyochi, *Member, IEEE*

***Abstract*—A raw image captured by a color filter array (CFA), such as a Bayer pattern, is usually compressed after demosaicing with some processings (denoising, deblurring, tone-mapping, and so on). However, since photographers, designers, and high-end users prefer to work with the raw image sampled by CFA (referred to as "raw image") directly, a raw image should be compressed before demosaicing. For effective raw image compression, this study introduces variable macropixel spectral-spatial transforms (VMSSTs), that can successfully decorrelate not only Bayer raw images but any other pure-color (RGB) ones. The proposed VMSSTs are designed by the following two steps: 1) intra-color decorrelation and 2) inter-color decorrelation. In lossless compression with JPEG 2000, compared with methods which do not use transforms, the VMSSTs reduced the average bitrates of three types of CFAs: from approximately 0.09 to 0.12 bpp for the modified Bayer CFA, from 0.25 to 0.65 bpp for the diagonal stripe CFA, and from 0.33 to 0.70 bpp for the Fujifilm X-Trans CFA due to their high color decorrelation efficiency. In addition, in lossy compression with JPEG 2000, compared with a rearranged method, the VMSSTs improved the average bitrates of the Bjøntegaard delta by around 3.97 %, 14.95 %, and 18.65 % for each CFA model, respectively. Although a data-dependent adaptive transformation, the Karhunen-Loève transform (KLT), showed the best performance in lossy compression, the introduced VMSSTs have shown performances comparable to those of the KLT in lossless compression, despite their simple structures.**

***Index Terms*—Color filter array, color transform, macropixel, pure-color, raw image, spectral-spatial transform.**

I. Introduction

In the image acquisition procedure, image data is first captured by a color filter array (CFA), then it is converted to RGB full-color images with demosaicing. The most popular CFA is a Bayer CFA [1] consisting of 2×2 macropixels with an $\mathrm{RG^2B}$ (red, two greens, and blue) CFA, as shown in Fig. 1(a). Other pure-color (RGB) CFAs consisting of only certain red, green, and blue components have been introduced, for example, modified Bayer CFA [2], diagonal stripe CFA [2], and Fujifilm X-Trans CFA [3] (Fig. 1(b)-(d)). Moreover, various non-pure-color (panchromatic) CFAs have been presented as alternatives to the RGB CFAs to obtain higher accuracy images, for example, Kodak CYYM (cyan, two yellows, and magenta) [4] CFA, Sony RGBE (red, green, blue, and emerald like cyan) [5] CFA, Kodak RGBW (red, green, blue, and white) [6] CFA, and Hirakawa's CFA [7]. This study focuses on only RGB CFAs for simplicity.

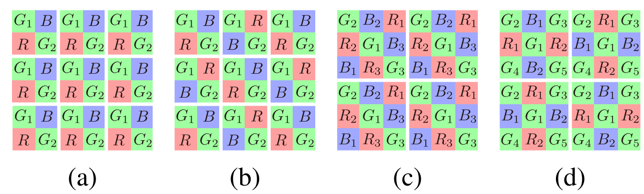

Fig. 1: RGB CFA types (each pixel set framed with a white square is a macropixel): (a) Bayer, (b) modified Bayer CFA, (c) diagonal stripe CFA, and (d) X-Trans CFA.

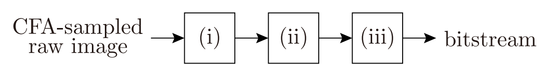

Fig. 2: Diagram of raw image compression: (i) color decorrelation, (ii) grouping components, and (iii) encoding parts.

Photographers, designers, and high-end users prefer that the raw images sampled by CFA (hereinafter referred to as "raw images") are not pre-processed. Many studies [8–17] have presented methods of compressing raw images before processing. With compression of full-color images, the spectral components of a pixel with a high inter-color correlation are generally decorrelated with a color transformation, converting, as a preprocessing step, the initial data from RGB color space into YUV color space (luma and two chroma components). Similarly, in the case of the compression of a raw image, the color components should also be decorrelated as shown in Fig. 2. We refer [12–17] for further discussion on the topic. Our previous work [17] indicated that SSTs can be represented by cascading discrete wavelet transforms, such as the Haar, 5/3-tap, and 9/7-tap wavelet transforms. The wavelet-based SST (WSST) in [17] covers other SSTs [12–16]; that is, the existing SSTs are obtained by bypassing parts of the wavelet transforms in the WSSTs and/or by replacing them with Haar transforms. Among them, the macropixel SST (MSST) [13], constructed from only three Haar transforms in the smallest pixel pattern composing a CFA (macropixel), has lower complexity than WSSTs with other wavelet transforms because a Haar transformation can simply be performed with an adder, a subtracter, and a bit shift.

Although the existing SSTs effectively work for Bayer raw images, they would not work for other types of CFAs, because design methods of those transforms significantly depend on

T. Suzuki is with the Faculty of Engineering, Information and Systems, University of Tsukuba, Tsukuba 305-8573, Japan (e-mail: taizo@cs.tsukuba.ac.jp).

S. Kyochi is with the Department of Information and Media Engineering, The University of Kitakyushu, Kitakyushu 808-0135, Japan (e-mail: s-kyochi@kitakyu-u.ac.jp).

the configuration of a Bayer CFA. One of the possible ways is to apply a data-dependent adaptive transformation, the Karhunen-Loève transform (KLT). However, this approach requires additional computational/bit cost to derive the KLT matrix and transmit it to the decoder.

This study introduces variable MSSTs (VMSSTs) for arbitrary RGB raw images, not constrained by a Bayer CFA. The novelties of this study are summarized as follows:

1. We propose a universal design approach for the VMSSTs that consist of two steps: 1) intra-color decorrelation and 2) inter-color decorrelation.
2. To easily achieve lossy-to-lossless compression, we design the VMSSTs with lifting-based Haar transforms.

Despite of their simple structures, the experiments at compression with the VMSSTs and JPEG 2000 [18] show the VMSSTs achieves high performance for non-Bayer RGB raw images.

Notation: Boldface letters represent vectors and matrices and non-boldface ones represent scalars. $\mathbf{I}$, $\mathbf{J}$, $\mathbf{O}$, $\mathrm{diag}(\mathbf{M}_0, \mathbf{M}_1, \cdots)$, and superscript $\cdot^\top$ denote a 2×2 identity matrix, 2×2 reversal (permutation) matrix, zero matrix, block diagonal matrix with $\mathbf{M}_n \in \mathbb{R}^{N_n\times N_n}$ ($N_n \geq 1$), and transpose of a matrix/vector, respectively.

II. Review and Definitions

A. Haar Transform

The Haar transform $\mathbf{H}$, the simplest wavelet transform, is expressed in [19] as follows:

$$\left[M_\mathrm{x}, D_\mathrm{x}\right]^\top = \mathbf{H}\left[X_1, X_2\right]^\top, \tag{1}$$

where

$$\mathbf{H} = \begin{bmatrix} 1/2 & 1/2 \\ -1 & 1 \end{bmatrix} = \begin{bmatrix} 1 & 1/2 \\ 0 & 1 \end{bmatrix}\begin{bmatrix} 1 & 0 \\ -1 & 1 \end{bmatrix}. \tag{2}$$

The above means that the calculation simply consists of calculating the "mean" M_x and "difference" D_x between the two input signals X_1 and X_2. By using lifting steps (shown in (2)) with a rounding operation, the Haar transform can be an integer-to-integer reversible transform, which is necessary for lossless compression. Moreover, the lifting-based Haar transform can be implemented by only an adder, a subtracter, and a bit shift.

B. Reversible Color Transform (RCT)

As a preprocessing, a color transform is generally implemented to decorrelate the RGB components R, G, and B of a full-color image. Conventional color transforms are classified into reversible and irreversible classes. Since the application of this study is both lossless and lossy raw image compression, we focus on reversible color transforms (RCTs). A typical RCT is the YCoCg-based RCT (YCoCg-R) [20], which changes a full-color image from RGB color space into YCoCg color space composed of a luma component Y, a chrominance orange component C_o, and a chrominance green component C_g. The YCoCg-R $\mathbf{T}_\mathrm{ycocg}$ is composed of only two Haar transforms in (2) as follows:

$$\left[Y, C_\mathrm{o}, C_\mathrm{g}\right]^\top = \mathbf{T}_\mathrm{ycocg}\left[G, B, R\right]^\top, \tag{3}$$

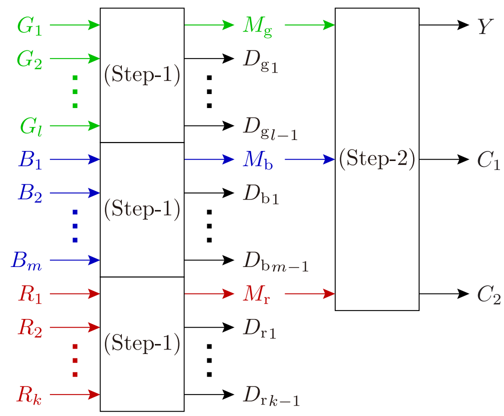

Fig. 3: VMSST in a macropixel: (Step-1) intra-color decorrelation and (Step-2) inter-color decorrelation.

where

$$\mathbf{T}_\mathrm{ycocg} = \mathrm{diag}(1, \mathbf{J}) \cdot \mathrm{diag}(\mathbf{HJ}, 1) \cdot \mathrm{diag}(1, \mathbf{H}). \tag{4}$$

As described in Section II-A, we can consider that the transform has very low complexity because it is composed of only two Haar transforms.

C. Macropixel Spectral-Spatial Transform (MSST)

This study focuses on MSST [13], which changes a Bayer raw image from RG^{2}B color space to YDgCoCg color space, where D_g means the difference green component. The transform is implemented within a 2×2 macropixel consisting of RG^{2}B components R, G_1, G_2, and B in a Bayer CFA. The conventional MSST $\mathbf{S}_\mathrm{msst}$ is represented as follows:

$$\left[Y, D_\mathrm{g}, C_\mathrm{o}, C_\mathrm{g}\right]^\top = \mathbf{S}_\mathrm{msst}\left[G_1, G_2, B, R\right]^\top, \tag{5}$$

where

$$\mathbf{S}_\mathrm{msst} = \mathbf{P}_2 \cdot \mathrm{diag}(\mathbf{H}, \mathbf{I}) \cdot \mathbf{P}_1 \cdot \mathrm{diag}(\mathbf{H}, \mathbf{H}). \tag{6}$$

Here, $\mathbf{P}_1$ and $\mathbf{P}_2$ are permutation matrices:

$$\mathbf{P}_1 = \begin{bmatrix} 0 & 0 & 1 & 0 \\ 1 & 0 & 0 & 0 \\ 0 & 1 & 0 & 0 \\ 0 & 0 & 0 & 1 \end{bmatrix}, \quad \mathbf{P}_2 = \begin{bmatrix} 1 & 0 & 0 & 0 \\ 0 & 0 & 1 & 0 \\ 0 & 0 & 0 & 1 \\ 0 & 1 & 0 & 0 \end{bmatrix}. \tag{7}$$

Again, it has very low complexity because it is composed of only three Haar transforms.

III. Variable Macropixel Spectral-Spatial Transforms (VMSSTs)

A. Proposed Framework: Intra- and Inter-color Decorrelations

The proposed VMSSTs for arbitrary RGB raw images are composed of the following two steps (see Fig. 3).

[(Step-1) Intra-color decorrelation] The color components $X_n = (R_n, G_n, B_n)$ ($n \in \mathbb{N}$ depending on each color) in a macropixel are separately changed into the mean color components $M_\mathrm{x} = (M_\mathrm{r}, M_\mathrm{g}, M_\mathrm{b})$ and the difference color components $D_{\mathrm{x}n} = (D_{\mathrm{r}n}, D_{\mathrm{g}_n}, D_{\mathrm{b}n})$ by using Haar transforms $\mathbf{H}$. Although the intra-color decorrelation allows not only Haar transforms but also any other transform, we selected Haar transforms to achieve a simpler structure for each CFA type. Note that if n for a color component X_n in each macropixel is 1 ($n = 1$), the n is omitted and the mean and difference color components are set to $M_\mathrm{x} = X$ and D_x : N/A.

[(Step-2) Inter-color decorrelation] The mean color components M_x in a macropixel are changed into a luma component Y and two chroma components U and V with an RCT $\mathbf{T}_\mathrm{yuv}$:

$$\left[Y, U, V\right]^\top = \mathbf{T}_\mathrm{yuv} \left[M_\mathrm{g}, M_\mathrm{b}, M_\mathrm{r}\right]^\top . \tag{8}$$

For the RCT $\mathbf{T}_\mathrm{yuv}$, we can select not only YCoCg-R $\mathbf{T}_\mathrm{ycocg}$, but also any other RCT such as the YCbCr-based RCT used in JPEG 2000. This study uses the YCoCg-R $\mathbf{T}_\mathrm{ycocg}$, which consists only of the Haar transforms.

1) Revisit of MSST for Bayer Raw Images: The conventional MSST [13] can also be considered as an example of the proposed VMSSTs. To be specific, we can reorganize the conventional MSST for Bayer raw images in (6) into the following two steps using the YCoCg-R $\mathbf{T}_\mathrm{ycocg}$ in (4):

$$\mathbf{S}_\mathrm{msst} = \underbrace{\mathrm{diag}(\mathbf{J}, \mathbf{I}) \cdot \mathrm{diag}(1, \mathbf{T}_\mathrm{ycocg})}_{\text{(Step-2)}} \cdot \underbrace{\mathrm{diag}(\mathbf{JH}, \mathbf{I})}_{\text{(Step-1)}} . \tag{9}$$

[(Step-1) Intra-color decorrelation] Two green components G_1 and G_2 in a macropixel are changed into the mean green component M_g and the difference green component D_g by using a Haar transform $\mathbf{H}$:

$$\left[M_\mathrm{g}, D_\mathrm{g}\right]^\top = \mathbf{H} \left[G_1, G_2\right]^\top . \tag{10}$$

[(Step-2) Inter-color decorrelation] The red component R, mean green component M_g, and blue component B in a macropixel are changed into the luma component Y, chrominance orange component C_o, and chrominance green component C_g by using the YCoCg-R $\mathbf{T}_\mathrm{ycocg}$:

$$\left[Y, C_\mathrm{o}, C_\mathrm{g}\right]^\top = \mathbf{T}_\mathrm{ycocg} \left[M_\mathrm{g}, B, R\right]^\top . \tag{11}$$

B. Application for Non-Bayer RGB Raw Images

This subsection shows applications of intra- and inter-color decorrelations for non-Bayer RGB raw images. In this work, we modify the intra-color decorrelation according to the CFA type, and do not modify the inter-color decorrelation. Thus, we show only (Step-1) part for each CFA type.

1) For Modified Bayer CFA: We can consider that a modified Bayer CFA [2] to be composed of 4×4 macropixels with four red components, eight green components, and four blue components as shown in Fig. 1(b). For low complexity, we subdivide a 4×4 macropixel into four 2×2 macropixels (submacropixels) with RG^{2}B components R, G_1, G_2, and B and implement the VMSST in each of the 2×2 submacropixels. Since a submacropixel is the same or the transposed version of the other submacropixels, it is sufficient to design the intra-color decorrelation for a submacropixel. For (Step-1) in the VMSST, the mean color components M_x and the difference color components D_x are calculated using a Haar transform $\mathbf{H}$ for only the two green components G_1 and G_2:

$$\left[M_\mathrm{g}, D_\mathrm{g}\right]^\top = \mathbf{H} \left[G_1, G_2\right]^\top , \; M_\mathrm{r} = R, \; M_\mathrm{b} = B, \tag{12}$$

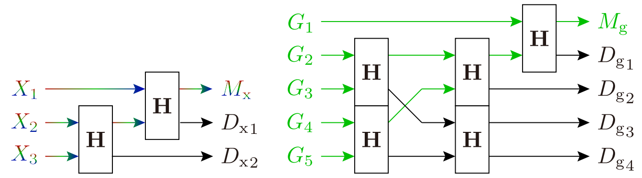

(a) (b)

Fig. 4: Examples of intra-color decorrelation in a macropixel: (a) for diagonal stripe CFA and (b) for X-Trans CFA.

where D_r and D_b : N/A. It is clear that any VMSST for arbitrary RGB raw images consisting of 2×2 macropixels with RG^{2}B components R, G_1, G_2, and B is completely the same as the revisited MSST for Bayer raw images as shown in Section III-A1.

2) For Diagonal Stripe CFA: A diagonal stripe CFA [2] can be constructed from 3×3 macropixels with three components in each color, as shown in Fig. 1(c). For (Step-1) in the VMSST, the mean color components M_x and the difference color components $D_{\mathrm{x}n}$ are calculated using two Haar transforms for each of the color components X_1, X_2, and X_3 (see Fig. 4(a)):

$$\left[M_\mathrm{x}, D_{\mathrm{x}1}, D_{\mathrm{x}2}\right]^\top = \mathrm{diag}(\mathbf{H}, 1) \cdot \mathrm{diag}(1, \mathbf{H}) \cdot \left[X_1, X_2, X_3\right]^\top . \tag{13}$$

3) For X-Trans CFA: An X-Trans CFA has 6×6 macropixels with eight red components, 20 green components, and eight blue components as shown in Fig. 1(d). However, we subdivide a 6×6 macropixel into four 3×3 submacropixels with R^{2}G^{5}B^2 components R_1, R_2, G_1, G_2, G_3, G_4, G_5, B_1, and B_2 and implement the VMSST in each of the 3×3 submacropixels as in the case of the modified Bayer CFA described in Section III-B1. For (Step-1) in the VMSST, the mean color components M_x and the difference color components $D_{\mathrm{x}n}$ are calculated using a Haar transform $\mathbf{H}$ for each of two red components R_1 and R_2 and two blue components B_1 and B_2:

$$\left[M_\mathrm{r}, D_\mathrm{r}\right]^\top = \mathbf{H} \left[R_1, R_2\right]^\top , \; \left[M_\mathrm{b}, D_\mathrm{b}\right]^\top = \mathbf{H} \left[B_1, B_2\right]^\top , \tag{14}$$

and five Haar transforms $\mathbf{H}$ for five green components G_1, G_2, G_3, G_4, and G_5 (see Fig 4(b)):

$$\begin{aligned} &\left[M_\mathrm{g}, D_{\mathrm{g}_1}, D_{\mathrm{g}_2}, D_{\mathrm{g}_3}, D_{\mathrm{g}_4}\right]^\top \\ &= \mathrm{diag}(\mathbf{H}, \mathbf{J}, 1) \cdot \mathrm{diag}(1, \mathbf{H}, \mathbf{H}) \cdot \mathrm{diag}(\mathbf{I}, \mathbf{J}, 1) \\ &\quad \cdot \mathrm{diag}(1, \mathbf{H}, \mathbf{H}) \left[G_1, G_2, G_3, G_4, G_5\right]^\top . \end{aligned} \tag{15}$$

IV. Non-Bayer RGB Raw Image Compression

We evaluated the proposed VMSSTs in terms of lossless bitrate [bpp] and bitrate of the Bjøntegaard delta (BD-rate) [%] in non-Bayer RGB raw image compression. We used three methods as conventional methods. The first method, "Direct," directly inputs a raw image to the encoding part in Fig. 2(iii) (bypassing the color decorrelation and grouping components parts in Fig. 2(i) and (ii)). The second method, "ReRGB," inputs a raw image to the grouping components and encoding parts in Fig. 2(ii) and (iii) (bypassing the color decorrelation

TABLE I: Non-Bayer RGB raw image compression results.

Test Images	Modified Bayer CFA [2] Direct	ReRGB	KLT	VMSST	Diagonal Stripe CFA [2] Direct	ReRGB	KLT	VMSST	X-Trans CFA [3] Direct	ReRGB	KLT	VMSST
Lossless compression results (lossless bitrate [bpp], where the cases of KLT are not true lossless compressions)												
Akademie	11.55	11.58	11.43	**11.41**	12.24	11.90	**11.44**	11.56	12.24	11.94	11.47	**11.46**
Arri	10.77	10.89	10.68	**10.62**	11.52	11.29	**10.73**	10.87	11.52	11.33	**10.76**	**10.76**
Church	**10.07**	10.43	10.11	10.09	10.64	10.83	**10.20**	10.33	10.65	10.82	**10.19**	10.24
⋮	⋮	⋮	⋮	⋮	⋮	⋮	⋮	⋮	⋮	⋮	⋮	⋮
Pool	11.07	11.26	**11.05**	**11.05**	11.53	11.48	**11.02**	11.14	11.53	11.52	**11.04**	11.07
Siegestor	10.62	**10.40**	10.48	10.50	10.97	10.37	10.39	**10.32**	10.80	10.31	10.26	**10.24**
Average	10.70	10.67	**10.58**	**10.58**	11.25	10.85	**10.56**	10.60	11.22	10.85	**10.52**	**10.52**
Lossy compression results (BD-rate [%] compared with Direct in 0.125-1.00 bpp)												
Akademie	–	-47.23	**-61.03**	-47.13	–	-56.91	**-80.61**	-62.34	–	-64.74	**-84.69**	-72.40
Arri	–	-23.86	**-51.37**	-38.14	–	-6.66	**-68.25**	-34.17	–	-12.31	**-67.65**	-45.76
Church	–	-24.46	**-61.57**	-48.65	–	17.99	**-65.59**	-27.16	–	14.50	**-68.73**	-34.65
⋮	⋮	⋮	⋮	⋮	⋮	⋮	⋮	⋮	⋮	⋮	⋮	⋮
Pool	–	-23.82	**-52.94**	-37.40	–	7.31	**-64.43**	-20.35	–	6.68	**-66.12**	-33.13
Siegestor	–	**-50.87**	-47.75	-34.57	–	-67.75	**-71.61**	-61.15	–	-57.34	**-64.92**	-49.88
Average	–	-37.59	**-54.57**	-41.56	–	-35.42	**-73.51**	-50.37	–	-34.72	**-72.55**	-53.37

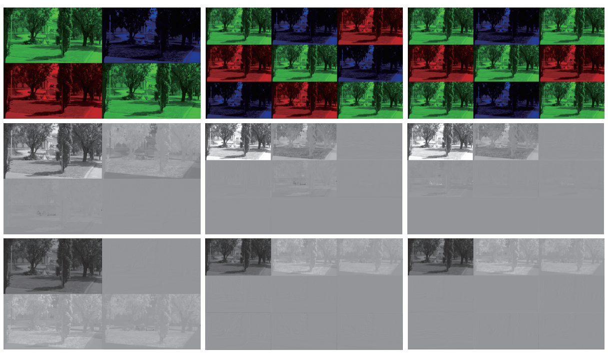

Fig. 5: Rearranged and decorrelated non-Bayer RGB raw images (*Akademie*): (left to right) modified Bayer CFA, diagonal stripe CFA, and X-Trans CFA, (top to bottom) ReRGB, KLT, and VMSST.

part in Fig. 2(i)). The third method, "KLT," inputs a raw image to all parts in Fig. 2, where the KLT is used as a color decorrelation.[1] According to the previous works [13] and [17], we chose JPEG2000 codec as a coder (we used the `MATLAB` built-in function `imwrite.m` without any modification).[2] As test images, we used ten 2880×1620 RGB full-color images with a 16-bit dynamic range in each pixel from [23]. We selected the modified Bayer CFA [2], diagonal stripe CFA [2], and X-Trans CFA [3] for arbitrary RGB CFA types of raw images. To simulate the raw images, we subsampled the test images in accordance with the CFA types in Fig. 1(b)-(d) and reduced their dynamic range from 16 to 14 bits because the actual sensor data often had only about 10 to 14-bit resolution at most. Since the decorrelated color components except for the luma component Y had both positive and negative values and the JPEG 2000 codec does not allow input signals with negative values, we transmitted the transformed coefficients, which had 15-bit positive values by adding 2^{14}, on the encoder side and reconstructed the images after subtracting 2^{14} on the decoder side.

Figure 5 shows the rearranged and decorrelated images of the *Akademie*. It is clear that the color components were highly decorrelated by the KLT and the VMSSTs. Table I shows the lossless bitrates and the BD-rates with JPEG 2000 for three types of non-Bayer RGB raw images. In lossless compression, the VMSSTs reduced the average bitrates by around 0.09–0.12 bpp, 0.25–0.65 bpp, and 0.33–0.70 bpp for each CFA type, respectively, compared with the case of "Direct" and "ReRGB" (no color decorrelation). Also, the VMSSTs showed comparable performance with the KLT despite their simple structures composed of Haar transforms. Moreover, in lossy compression, the VMSSTs improved the average BD-rates by around 3.97 %, 14.95 %, and 18.65 % for each CFA type, respectively, compared with the case of "ReRGB." In particular, larger improvements were seen in the case of the 3×3 macropixel/submacropixel, such as in diagonal stripe CFA and X-Trans CFA, than in the 2×2 submacropixel case, such as in modified Bayer CFA. We consider that there is a trade-off between the effectiveness of color decorrelation using nearby components and the complexity depending on the size of the macropixel. Although the proposed VMSSTs could not achieve comparable performance with the KLT in lossy compression, it can provide both lossless and lossy compression with fewer computational operations.[3]

V. Conclusion

We presented VMSSTs for arbitrary RGB raw images, not constrained by a Bayer CFA. The transforms were derived by reformulating the conventional MSST for the most popular Bayer raw images as the following two steps: 1) intra-color decorrelation and 2) inter-color decorrelation. The experiments at compression with the VMSSTs and JPEG 2000 showed good compression performance because of the high effectiveness of color decorrelation.

[1]Note that raw images cannot be encoded/decoded losslessly by the KLT, because the KLT is not a reversible transform. We just show the performance of the KLT in lossless compression as reference results.

[2]Other codecs such as JPEG [21] and JPEG XR [22] can also be applied.

[3]The KLT matrix should be calculated and transmitted to the decoder.

REFERENCES

[1] B. E. Bayer, "Color imaging array," 1976, U.S. Patent 3 971 065.

[2] R. Lukac and K. N. Plataniotis, "Color filter array: Design and performance analysis," *IEEE Trans. Consum. Electron.*, vol. 51, no. 4, pp. 1260–1267, Nov. 2005.

[3] "Fujifilm X-Trans sensor technology," *Fujifilm UK Official Website [Online]*, July 2003, Available: https://www.fujifilm.eu/uk/products/digital-cameras/model/x-pro1/features-4483/aps-c-16m-x-trans-cmos.

[4] "Kodak DCS620x review," *Digital Photography Review [Online]*, June 2000, Available: http://www.dpreview.com/reviews/kodakdcs620x/.

[5] "Sony announce new RGBE CCD," *Digital Photography Review [Online]*, July 2003, Available: http://www.dpreview.com/articles/1471104084/sonyrgbeccd.

[6] E. T. Chang, "High-sensitivity infrared color camera," 2005, U.S. Patent 20070145273.

[7] K. Hirakawa and P. J. Wolfe, "Spatio-spectral color filter array design for optimal image recovery," *IEEE Trans. Image Process.*, vol. 17, no. 10, pp. 1876–1890, Oct. 2008.

[8] C. C. Koh, J. Mukherjee, and S. K. Mitra, "New efficient methods of image compression in digital cameras with color filter array," *IEEE Trans. Consum. Electron.*, vol. 49, no. 4, pp. 1448–1456, Nov. 2003.

[9] K.-H. Chung and Y.-H. Chan, "A lossless compression scheme for Bayer color filter array images," *IEEE Trans. Image Process.*, vol. 17, no. 2, pp. 134–144, Feb. 2008.

[10] S. Kim and N. I. Cho, "Lossless compression of color filter array images by hierarchical prediction and context modeling," *IEEE Trans. Circuit. Syst. Video Technol.*, vol. 24, no. 6, pp. 1040–1046, June 2014.

[11] M. Lakshmia, J. Senthilkumarb, and Y. Suresh, "Visually lossless compression for Bayer color filter array using optimized vector quantization," *Appl. Soft Comput.*, vol. 46, pp. 1030–1042, Sep. 2016.

[12] N. Zhang and X. Wu, "Lossless compression of color mosaic images," *IEEE Trans. Image Process.*, vol. 15, no. 6, pp. 1379–1388, June 2006.

[13] H. S. Malvar and G. J. Sullivan, "Progressive-to-lossless compression of color-filter-array images using macropixel spectral-spatial transformation," in *Proc. DCC'12*, Snowbird, UT, Apr. 2012, pp. 3–12.

[14] M. Hernández-Cabronero, M. W. Marcellin, I. Blanes, and J. Serra-Sagristà, "Lossless compression of color filter array mosaic images with visualization via JPEG 2000," *IEEE Trans. Multimedia*, vol. 20, no. 2, pp. 257–270, Feb. 2018.

[15] Y. Lee, K. Hirakawa, and T. Q. Nguyen, "Camera-aware multi-resolution analysis for raw image sensor data compression," *IEEE Trans. Image Process.*, vol. 27, no. 6, pp. 2806–2817, June 2018.

[16] T. Richter and S. Fößel, "Bayer pattern compression with JPEG XS," in *Proc. ICIP'19*, Taipei, Taiwan, Oct. 2019, pp. 3177–3181.

[17] T. Suzuki, "Wavelet-based spectral-spatial transforms for CFA-sampled raw camera image compression," *IEEE Trans. Image Process.*, vol. 29, no. 1, pp. 433–444, Dec. 2020.

[18] A. Skodras, C. Christopoulis, and T. Ebrahimi, "The JPEG2000 still image compression standard," *IEEE Signal Process. Mag.*, vol. 18, no. 5, pp. 36–58, Sep. 2001.

[19] W. Sweldens, "The lifting scheme: A construction of second generation wavelets," *SIAM J. Math. Anal.*, vol. 29, no. 2, pp. 511–546, 1998.

[20] H. S. Malvar, G. J. Sullivan, and S. Srinivasan, "Lifting-based reversible color transformations for image compression," in *Proc. SPIE Appl. Digit. Image Process. XXXI*, San Diego, CA, Aug. 2008, vol. 7073, pp. 1–10.

[21] G. K. Wallace, "The JPEG still picture compression standard," *IEEE Trans. Consum. Electr.*, vol. 38, no. 1, pp. xviii–xxxiv, Feb. 1992.

[22] F. Dufaux, G. J. Sullivan, and T. Ebrahimi, "The JPEG XR image coding standard," *IEEE Signal Process. Mag.*, vol. 26, no. 6, pp. 195–199, 204, Nov. 2009.

[23] S. Andriani, H. Brendel, T. Seybold, and J. Goldstone, "Beyond the Kodak image set: A new reference set of color image sequences," in *Proc. ICIP'13*, Melbourne, Australia, Sep. 2013, pp. 2289–2293.